Consensus Control for Vehicular Platooning With Velocity Constraints

Jeroen C. Zegers, Elham Semsar-Kazerooni, Jeroen Ploeg, Nathan van de Wouw, and Henk Nijmeijer, *Fellow, IEEE*

***Abstract*— In this paper, a distributed consensus control approach for vehicular platooning systems is proposed. In formalizing the underlying consensus problem, a realistic vehicle dynamics model is considered and a velocity-dependent spacing policy between two consecutive vehicles is realized. As a particular case, the approach allows to consider bidirectional vehicle interaction, which improves the cohesion between vehicles in the platoon. Exponential stability of the platoon dynamics is evaluated, also in the challenging scenario in which a limitation on the velocity of one of the vehicles in the platoon is introduced. The theoretical results are experimentally validated using a three-vehicle platoon consisting of (longitudinally) automated vehicles equipped with wireless intervehicle communication and radar-based sensing.**

***Index Terms*— Consensus, distributed control, intelligent transportation systems, vehicular platooning, velocity constraint.**

I. Introduction

THE societal demand to have clean, safe, and efficient traffic systems on one hand and the need to improve these systems to an adequate capacity level to prevent traffic jams on the other hand have created large interest in the concept of automated driving in recent years. Moreover, the advances in computation, sensing, and communication technology supported and empowered this interest in automated traffic systems. The overall goal of automated driving is to optimize traffic throughput, reduce overall exhaust emission [1], and increase traffic safety [2].

Cooperative adaptive cruise control (CACC) systems potentially contribute to such automation of on-road traffic. CACC systems, of which particular implementations are described in [3]–[6], are used for the control of a platoon of vehicles. These systems employ wireless vehicle-to-vehicle communication, in addition to on-board measurements, to allow for driving at small intervehicle distances. While achieving short-distance vehicle following, string stable platoon behavior, i.e., disturbance attenuation along the platoon, is desired as well [4]. Driving with such short following distance can significantly improve the road traffic throughput.

An example of a CACC implementation, which guarantees a string stable behavior, is described in [4] and [5], where the underlying interaction topology is a one-vehicle look-ahead topology. That is, each vehicle only uses the information of its direct predecessor. Although this connectivity structure is useful and practical in many applications, in some cases, is it desired to have more flexibility in the design of the interaction topology between the vehicles in a platoon. In particular, in a one-vehicle look-ahead topology, there is no possibility to inform the leading vehicles of the performance of the followers. In contrast, using information of the follower vehicles can potentially improve the platoon cohesion. To support this statement, envision a real-life scenario in which the vehicles in a platoon have different limitations in terms of velocity or acceleration. In particular, heavy-duty vehicles may have a difference in weight due to the load variations leading to distinct velocity and acceleration constraints. Such differences in velocity or acceleration constraints may lead to an undesired platoon breakup in case of a unidirectional interaction topology between the platoon vehicles. The platoon cohesion is likely to be improved by a bidirectional scheme, and however, such a scheme also has adverse effects, e.g., tight margins on string stability [25], [29].

This may be solved by formalizing the platoon control problem in a framework offering more flexibility in terms of the interaction topology, e.g., by using a bidirectional interaction topology. To this end, a platoon of vehicles can be viewed as an interconnected network of dynamic vehicular systems interacting through an underlying communication and sensing network. Since these networked vehicles aim at a synchronized behavior in terms of identical velocity and intervehicle distances, the platoon control problem aligns well with the existing system-theoretic frameworks, such as consensus seeking [7] and flocking [8], see also the overview of distributed multiagent coordination in [9] and the recent overview of vehicular platoon control under the four-component framework [27].

In recent work, the platoon control problem has indeed been cast into a distributed consensus control framework [10]–[12], [25], [26]. In most of these papers, a constant-distance spacing policy between two consecutive vehicles in the platoon is considered. However, in terms of traffic throughput, safety, and disturbance attenuation, a constant-distance spacing policy is not preferable [13], [14]. Furthermore, the robustness to vehicle actuator faults or bounded control inputs, which can be seen as limitations on the velocity

Manuscript received April 20, 2016; revised December 7, 2016 and June 6, 2017; accepted June 22, 2017. Date of publication July 11, 2017; date of current version August 6, 2018. Manuscript received in final form June 22, 2017. Recommended by Associate Editor A. Serrani. *(Corresponding author: Jeroen C. Zegers.)*

J. C. Zegers, E. Semsar-Kazerooni, and J. Ploeg are with the Integrated Vehicle Safety Department, TNO, 5700 AT Helmond, The Netherlands (e-mail: jeroen.zegers@tno.nl; elham.semsarkazerooni@tno.nl; jeroen.ploeg@tno.nl).

N. van de Wouw and H. Nijmeijer are with the Department of Mechanical Engineering, Eindhoven University of Technology, 5612 AZ Eindhoven, The Netherlands, also with the Department of Civil, Environmental and Geo-Engineering, University of Minnesota, Minneapolis, MN USA, and also with the Delft Center for Systems and Control, Delft University of Technology, Delft, The Netherlands (e-mail: n.v.d.wouw@tue.nl; h.nijmeijer@tue.nl).

Digital Object Identifier 10.1109/TCST.2017.2720141

or acceleration, is investigated in [15]–[17]. However, in the study of actuator faults [15], temporary or periodic actuator faults are assumed. As a result, the group of agents will break up when the actuator fault is permanent. This is not the case for the approach developed in this paper.

In a previous paper of the authors, the vehicle following problem was modeled as a consensus seeking problem [18]. The contribution of this paper is the extension of these results to the case where platoon members are not homogenous in terms of their dynamical capabilities. Specifically, the focus is on solving the platoon cohesion problem when some of the platoon members have a limited velocity capability. Through an appropriate design of the local controllers as well as the adopted interaction topology, it is shown that the platoon can automatically identify this limitation and adapt its behavior to the vehicles with limited functionality.

In this paper, a longitudinal vehicle dynamics model as in [4], [12], [19], and [26] is adopted. This model includes the influence of the vehicle drive-line dynamics and is known to be a realistic model. Furthermore, the intervehicle spacing policy is considered to be velocity dependent in contrast to the work done in [10], [12], [25], and [26]. A formal analysis of the exponential stability of the entire platoon dynamics, subject to existence of constrained vehicles in the platoon, is provided. The performance of the networked control strategy is evidenced by a simulation-based case study, and practical feasibility is demonstrated using an experimental three-vehicle test setup.

The outline of this paper is as follows. Section II gives a brief overview of the preliminaries of consensus control and the problem formulation. In Section III, a distributed control approach is proposed for exponential stability of the platoon dynamics. In Section IV, a velocity constraint is introduced, and again exponential stability of the platoon dynamics is presented. The analytical result is verified by a simulation-based study in Section V. Section VI shows the results of a three-vehicle platoon practical feasibility study. Finally, Section VII presents the main conclusions.

II. Preliminaries and Problem Statement

A. Graph Theory

A way to model information exchange in a network of dynamical systems is by using the so-called graphs. A graph consists of a node (e.g., a vehicle) set $\mathcal{V} = \{1, \cdots, n\}$ and an edge set $\mathcal{E} \in \mathcal{V} \times \mathcal{V}$. In an *undirected graph*, the existence of an edge from node i to node j implicates the existence of an edge from node j to node i, i.e., the information link is bidirectional. In a *directed graph (or digraph)*, at least one pair of nodes has a unidirectional information link. An undirected graph is called *connected* if there is a path between any distinct pair of nodes via the edges of the graph, possibly via other nodes. For a digraph, a distinction is made between a graph being connected or *strongly* connected. A digraph is called strongly connected if there exists a path between any distinct pair of nodes via the graph's edges. A digraph is called connected, if there exists a path between any distinct pair of nodes when you replace all directed communication links in the graph by undirected communication links. A digraph contains a so-called *directed spanning tree* if there is at least one node having a directed path, via the graph's edges, to all other nodes. Such a node is called a root. The edge set $\mathcal{E}$ can be described by an adjacency matrix $G = [g_{ij}] \in \mathbb{R}^{n\times n}$ with $i, j \in \mathcal{V}$. If the edge set contains an edge from node j to node i, then element g_{ij} equals 1; g_{ij} equals 0 otherwise. Another fundamental matrix in a graph theory, which can be derived from the adjacency matrix G, is called the Laplacian matrix $L = [l_{ij}] \in \mathbb{R}^{n\times n}$. This matrix is defined as

$$l_{ii} = \sum_{j=1}^{n} g_{ij} \text{ and } l_{ij} = -g_{ij} \quad i \neq j. \tag{1}$$

The Laplacian matrix L satisfies the conditions

$$l_{ij} \leq 0 \quad i \neq j \text{ and } \sum_{j=1}^{n} l_{ij} = 0. \tag{2}$$

For an undirected graph, the Laplacian matrix L is symmetric positive semidefinite. However, for a digraph, the symmetry property does not hold. When a digraph contains a directed spanning tree or when an undirected graph is connected, the Laplacian matrix L has only one eigenvalue being zero. This single zero eigenvalue is associated with a right eigenvector $w \in \mathbb{R}^n$ of the Laplacian matrix satisfying

$$w := \alpha \, (1 \ \cdots \ 1)^T \tag{3}$$

where $\alpha \neq 0$. In addition to a Laplacian matrix L, which describes the topology of a network, a pinning matrix $P = [p_{ij}] \in \mathbb{R}^{n\times n}$ is defined as follows. The pinning matrix P is a diagonal matrix, which defines a pinning on one of the nodes in the network [20]. This pinning element "pins" the consensus state of all nodes in the network to a desired consensus state by putting an internal feedback on that specific node. The diagonal elements of the pinning matrix are either 0 or 1 and satisfy the following equation:

$$\sum_{i=1}^{n} p_{ii} = 1 \tag{4}$$

which implies that the states of only one node are pinned to a fixed value. In the method proposed in Section III, this means that one node will have an internal feedback in addition to the interaction due to the choice for the Laplacian matrix.

Next, an example of a simple consensus control strategy for a group of nodes (or systems) having single integrator dynamics is given to illustrate the principles of consensus control.

B. Consensus Control Law for Single-Integrator Dynamics

Consider a network of systems with dynamics given by

$$\dot{q}_i = u_i, \quad i \in \mathcal{V} \tag{5}$$

where $q_i(t) \in \mathbb{R}$ is the state of system i and $u_i(t) \in \mathbb{R}$ is the control input. A standard consensus control law for this group of systems, as proposed in [7] and [21], is given by

$$\boxed{u_i = -\sum_{j=1}^{n} g_{ij}(q_i - q_j), \quad i \in \mathcal{V}} \tag{6}$$

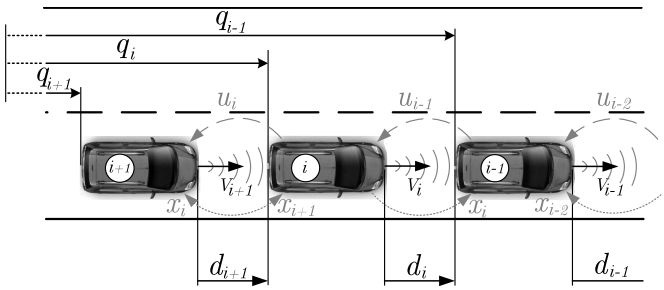

Fig. 1. Top view of a vehicle platoon. Dashed arrows: (fixed) communication topology of feedforward $u_{i-1}(t)$. Dotted arrows: (variable) communication topology for sharing information on the state $x_i(t)$.

where g_{ij} is the element of the adjacency matrix G describing the connectivity graph of the network. By introducing the lumped state vector $q(t) = (q_1(t) \ \dots \ q_n(t))^T$, the closed-loop dynamics, given by (5) and (6), are expressed as

$$\dot{q} = -Lq \tag{7}$$

where the relation between the elements of the adjacency matrix G and the Laplacian matrix L is as defined in (1). If the Laplacian matrix L has only one single eigenvalue equal to zero, i.e., the corresponding undirected graph is connected or the corresponding digraph contains a directed spanning tree, then it can be shown that consensus is reached among the n systems [21], that is

$$\lim_{t\to\infty} (q_i(t) - q_j(t)) = 0 \quad i \neq j. \tag{8}$$

Thus, all states exponentially converge to a common value, which depends on the initial conditions. The latter fact has a direct relation to the zero eigenvalue of the Laplacian.

When adding a pinning element, this common value is constrained to a desired value and, thus, does not depend on the initial conditions. Further explanation is given in Section II-C, where a more realistic dynamical model is considered relevant in the scope of vehicular platooning, and in addition, a velocity-dependent spacing policy is introduced.

C. Platoon Dynamics and Control Objective

Consider a platoon of n vehicles, as schematically shown in Fig. 1, where $x_i(t)$ is the consensus state vector, which will be defined in the following, $d_i(t)$ is the distance between vehicle i and its preceding vehicle $i-1$, and $q_i(t)$, $v_i(t)$, and $u_i(t)$ are the (rear-bumper) position, velocity, and control input, respectively, of vehicle i. Note that, in addition to the n vehicles, a virtual reference vehicle having index $i = 0$ is introduced, as is described in the following. The dotted arrows indicate the communication of the consensus state vector $x_j(t)$ from a vehicle j to a vehicle i, used for distributed consensus control, aiming to achieve closed-loop platoon stability. In addition, the dashed arrows indicate the communication of the control input $u_{i-1}(t)$ from vehicle $i-1$ to vehicle i, which represents a one-vehicle look-ahead feedforward as commonly used in CACC systems [4] and which will be described in the following in more detail. The following velocity-dependent spacing policy between two consecutive vehicles is desired:

$$\boxed{d_{\text{des},i}(t) = r + hv_i(t), \quad i \in \mathcal{V}} \tag{9}$$

where $r \geq 0$ and $h > 0$ are the standstill distance and the desired time gap, respectively, and $\mathcal{V} = \{1, \cdots, n\}$ is the set of all vehicles in the platoon. The spacing policy (9) is known to improve road efficiency [1], safety, and disturbance attenuation [13], [14]. The spacing error can then be defined as

$$\begin{aligned} e_i(t) &= d_i(t) - d_{\text{des},i}(t) \\ &= (q_{i-1}(t) - q_i(t) - l_v) - (r + hv_i(t)), \quad i \in \mathcal{V} \end{aligned} \tag{10}$$

where l_v is the vehicle length. As mentioned earlier, a virtual reference vehicle, having index $i = 0$, is introduced, such that the error $e_i(t)$ is also defined for the first vehicle in the platoon. The following longitudinal vehicle dynamics are adopted [4], [12], [19]:

$$\boxed{\begin{pmatrix} \dot{q}_i \\ \dot{v}_i \\ \dot{a}_i \end{pmatrix} = \underbrace{\begin{pmatrix} 0 & 1 & 0 \\ 0 & 0 & 1 \\ 0 & 0 & -\frac{1}{\tau} \end{pmatrix}}_{A} \begin{pmatrix} q_i \\ v_i \\ a_i \end{pmatrix} + \underbrace{\begin{pmatrix} 0 \\ 0 \\ \frac{1}{\tau} \end{pmatrix}}_{B} u_i(t-\phi), \quad i \in \{0\} \cup \mathcal{V}}$$

(11)

where τ is a positive constant representing the drive-line dynamics, ϕ is an actuator delay, and $a_i(t)$ is the vehicle acceleration. This dynamical model is a more realistic representation of the longitudinal vehicle dynamics in comparison with a double integrator dynamical model, as employed in [10] and [11]. It is assumed that τ is equal for all vehicles in the platoon, i.e., a homogeneous dynamic response of the vehicles is considered. Note that this does not necessarily mean that we consider a fully homogeneous platoon, since the velocity capabilities of the vehicles in the platoon may differ due to the velocity constraint, which will be introduced in the following. Also note that the virtual reference vehicle, i.e., vehicle $i = 0$, has the same dynamics as the other vehicles in the platoon, as defined in (11). As a result, in practice, the virtual reference vehicle could also be replaced by an actual leading vehicle. The control objective is to ensure that the closed-loop platoon dynamics exhibits an exponentially stable equilibrium for which it holds that

$$\lim_{t\to\infty} e_i(t) = 0, \quad i \in \mathcal{V} \tag{12}$$

for $u_0(t) = 0$. This control objective implies that all intervehicle distance errors $e_i(t)$ converge to zero when the velocity of the virtual reference vehicle $v_0(t)$ goes to a constant velocity $\bar{v}_0$ (which is the case for $u_0 = 0$). As a result from (10)–(12), it also holds that

$$\lim_{t\to\infty} v_i(t) = \bar{v}_0, \quad i \in \mathcal{V}. \tag{13}$$

The control objective, defined by (12) and (13), is achieved by a consensus-based control approach as explained in Section III.

In the presence of a velocity constraint $v_f(t) \leq v_{\max} < v_0(t)$ for a vehicle f, the control objective is to automatically adapt the platoon velocity toward the minimum of the virtual reference vehicle velocity $v_0(t)$ and the maximum velocity $v_{\max}$ of vehicle f, that is

$$\lim_{t\to\infty} v_i(t) = \min(\bar{v}_0, v_{\max}), \quad i \in \mathcal{V}. \tag{14}$$

This means that the platoon velocity converges to the desired velocity $\bar{v}_0$ imposed by the virtual reference vehicle, when

there is no velocity constraint, or the platoon velocity converges to $v_{\max}$ in case of a velocity constraint being present. This is explained in Section IV.

III. Exponential Stability of Nominal Consensus Framework

In this section, a distributed control approach to achieve the platoon control objectives (12) and (13), and conditions for exponential stability of the closed-loop platoon dynamics are proposed. For the sake of simplicity, the actuator delay ϕ in (11) is assumed to be equal to zero while designing the consensus-based controller. The impact of this delay is investigated in simulations and experiments in Sections V and VI. For the sake of readability, from now on, the time argument t is omitted. Let the error, as defined in (10), and its first and second time derivatives be stacked in the state vector

$$x_i = (e_i \quad \dot{e}_i \quad \ddot{e}_i)^T, \quad i \in \mathcal{V}. \tag{15}$$

Differentiating $\ddot{e}_i(t)$, while using (10) and (11), gives

$$\dddot{e}_i = -\frac{1}{\tau}\ddot{e}_i + \frac{1}{\tau}\left(u_{i-1} - u_i - h\dot{u}_i\right), \quad i \in \mathcal{V}. \tag{16}$$

By using (16), the following expression for the error dynamics can be obtained:

$$\dot{x}_i = Ax_i + B\left(u_{i-1} - u_i - h\dot{u}_i\right), \quad i \in \mathcal{V} \tag{17}$$

where A and B are defined as in (11), and $e_i(t)$ is defined in (10). Introducing the following precompensator on the vehicle input $u_i(t)$:

$$\dot{u}_i = -\frac{1}{h}u_i + \frac{1}{h}\left(u_{i-1} - \bar{u}_i\right), \quad i \in \mathcal{V} \tag{18}$$

with feedforward $u_{i-1}(t)$ and the new input $\bar{u}_i(t)$, where $u_{i-1}(t)$ is obtained by vehicle i through wireless communication, as is indicated (by the dashed arrows) in Fig. 1, yields the following error dynamics:

$$\dot{x}_i = Ax_i + B\bar{u}_i, \quad i \in \mathcal{V}. \tag{19}$$

Remark 1: The feedforward in terms of $u_{i-1}(t)$ in (18) is designed as to compensate for the aforementioned $u_{i-1}(t)$ term in the error dynamics in (17). This significantly improves the input disturbance attenuation properties of the platoon dynamics. This implies a one-vehicle look-ahead strategy for (only) the feedforward, but the following proposed approach gives freedom in communication topology used for the feedback design for the new input $\bar{u}_i(t)$.

Inspired by consensus control theory as explained in Section II-B, the following distributed controller is introduced for the new input $\bar{u}_i(t)$ in (18):

$$\bar{u}_i = -\sum_{j=1}^{n}\left(g_{ij}k^T(x_i - x_j)\right) - p_{ii}k^T x_i, \quad i \in \mathcal{V} \tag{20}$$

where $x_j(t)$ is obtained by vehicle i through additional communication links which are described by an adjacency matrix $G = [g_{ij}] \in \mathbb{R}^{n\times n}$. Moreover, p_{ii} represents the diagonal elements of a pinning matrix P (as explained in Section II-A) and $k^T = (k_p \; k_d \; k_{dd})$ is a controller gain vector. An example of a communication topology for realizing the distributed control term $\bar{u}_i(t)$ can be observed in Fig. 1 (indicated by the dotted arrows); however, the analysis given below is valid for any communication topology for the distributed controller.

Remark 2: The choice for the distributed control term for $\bar{u}_i(t)$ (the first term in (20)) is based on the desire to address interaction from follower vehicles and to have flexibility in the interaction between the vehicles in the platoon. The $p_{ii}k^T x_i$ term in (20) results in an internal feedback on one particular vehicle to ensure that all intervehicle distance errors converge to zero in the consensus equilibrium. Moreover, it must be noted that $p_{ii} = 0$ does not mean that the vehicle cannot access its own state or that its state is not used in the feedback, but it reflects a choice of the control structure. Note that when using the zero matrix for the adjacency matrix G and $p_{ii} = 1 \; \forall i \in \mathcal{V}$, the same unidirectional interaction as in [4] is obtained.

Let a lumped error state vector $X(t) \in \mathbb{R}^{3n\times 1}$ be defined as $X(t) := (x_1^T(t) \; \cdots \; x_n^T(t))^T$. Substitution of (20) into (19) results in the expression for the closed-loop error dynamics for the entire platoon as given in (24), as shown at the bottom of the next page, where the scalar elements l_{ij} are defined as in (1) and the scalar elements p_{ii} are either zero or one, satisfying (4). Now, let a lumped input state vector $U(t) \in \mathbb{R}^{n\times 1}$ be defined as $U(t) := (u_1(t) \; \cdots \; u_n(t))^T$. By substitution of (20) into (18) and by combining the result with (24), the following compact expression for the closed-loop platoon dynamics can be obtained:

$$\begin{pmatrix}\dot{X}\\ \dot{U}\end{pmatrix} = \begin{pmatrix} I_n \otimes A - \hat{L} \otimes Bk^T & O_{3n\times n} \\ \hat{L} \otimes \frac{k^T}{h} & \frac{1}{h}(I_{(-1),n} - I_n)\end{pmatrix}\begin{pmatrix}X\\ U\end{pmatrix} + \begin{pmatrix}O_{3n\times 1}\\ B_u\end{pmatrix}u_0 \tag{21}$$

where $\otimes$ denotes the Kronecker product, matrix $\hat{L} \in \mathbb{R}^{n\times n}$ is defined as $\hat{L} := L + P$, vector $B_u \in \mathbb{R}^{n\times 1}$ is defined as

$$B_u = \left(\frac{1}{h} \; 0 \; \cdots \; 0\right)^T \tag{22}$$

and vector $O_{3n\times 1} \in \mathbb{R}^{3n\times 1}$ and matrix $O_{3n\times n} \in \mathbb{R}^{3n\times n}$ are a zero vector and matrix, respectively. Furthermore, matrix $I_n \in \mathbb{R}^{n\times n}$ is an identity matrix and matrix $I_{(-1),n} \in \mathbb{R}^{n\times n}$ is defined as

$$I_{(-1),n} = \begin{pmatrix} 0 & \cdots & \cdots & \cdots & 0 \\ 1 & \ddots & & & \vdots \\ 0 & \ddots & \ddots & & \vdots \\ \vdots & & \ddots & \ddots & \vdots \\ 0 & \cdots & 0 & 1 & 0 \end{pmatrix}. \tag{23}$$

It can be observed that $u_0(t)$, which is the control input (or desired acceleration) of the virtual reference vehicle, is the only exogenous input to the platoon dynamics. Furthermore, note that, as a result of the precompensator in (18), the error dynamics (or X-dynamics) in (21) is independent of the time gap h.

In order to prove exponential stability of the closed-loop platoon dynamics (21), we first recall Lemma 1.

Lemma 1 [22]: The origin is an exponentially stable equilibrium of the dynamics

$$\dot{X} = (I_n \otimes A - \hat{L} \otimes Bk^T)X \tag{25}$$

if and only if all matrices

$$A - \lambda_i\{\hat{L}\}Bk^T, \quad i \in \mathcal{V} \tag{26}$$

are Hurwitz, where $\lambda_i\{\hat{L}\}$ is the ith eigenvalue of matrix $\hat{L}$.

Remark 3: Although it does not directly represent a constraint on the communication topology and the pinning element defined by $\hat{L}$, (26) implies that the pinning element should be applied to a vehicle that is the root of a directed spanning tree in the communication topology. As a result, the zero eigenvalue of the Laplacian L vanishes in $\hat{L}$.

Using this lemma, conditions for exponential stability can be derived, according to Theorem 1.

Theorem 1: The closed-loop platoon dynamics (21), with $\lambda_i\{\hat{L}\} \in \mathbb{R}^+$(positive real) $\forall i \in \mathcal{V}$ and $\tau > 0$, have an exponentially stable equilibrium (for $u_0 = 0$) if and only if the controller gain vector k of the controller defined by (18) and (20) satisfies

$$\begin{aligned} k_p &> 0 \\ k_d &> \frac{k_p \tau}{\min\limits_{i\in\mathcal{V}}\{\lambda_i\{\hat{L}\}k_{dd} + 1\}} \\ k_{dd} &> -\frac{1}{\max\limits_{i\in\mathcal{V}}\{\lambda_i\{\hat{L}\}\}}. \end{aligned} \tag{27}$$

Proof: Due to the lower block triangular structure of the closed-loop dynamics in (21), exponential stability can be assessed by evaluating the eigenvalues of the individual diagonal block matrices. It can easily be seen that the right lower matrix in the system matrix in (21) has only one single eigenvalue having algebraic multiplicity n, that is

$$\lambda_i\left\{\frac{1}{h}(I_{(-1),n} - I_n)\right\} = -\frac{1}{h}, \quad i \in \mathcal{V}. \tag{28}$$

Next, by using *Lemma 1*, it is known that the left upper matrix in the system matrix in (21) is Hurwitz if and only if all matrices (26) are Hurwitz. The characteristic polynomial of the matrix in (26), for A and B as given in (11), k as in (20), and $\hat{L}$ being the communication topology combined with the pinning element, is given by

$$\begin{aligned} &\det(\mu I_3 - (A - \lambda_i\{\hat{L}\}Bk^T)) \\ &\quad = \mu^3 + \frac{\lambda_i\{\hat{L}\}k_{dd} + 1}{\tau}\mu^2 + \frac{\lambda_i\{\hat{L}\}k_d}{\tau}\mu + \frac{\lambda_i\{\hat{L}\}k_p}{\tau} \end{aligned} \tag{29}$$

where $I_3 \in \mathbb{R}^{3\times 3}$ is an identity matrix and μ is an eigenvalue of matrix (26). According to the statement of the theorem, the eigenvalues of matrix $\hat{L}$ are positive real, i.e., $\lambda_i\{\hat{L}\} \in \mathbb{R}^+ \ \forall i \in \mathcal{V}$, and the drive-line dynamics constant satisfies $\tau > 0$. Employing the Routh–Hurwitz stability criterion [23] results in the necessary and sufficient conditions as given in (27) for all matrices in (26) being Hurwitz. These conditions are also necessary and sufficient for the left upper matrix in the system matrix in (21) being Hurwitz (see *Lemma 1*). As a result, the conditions in (27) are necessary and sufficient for the entire closed-loop dynamics (21) being exponentially stable. Hence, Theorem 1 is proven. □

Note that the stability conditions (27) do not depend on the time gap h. This is mainly achieved by the use of the precompensator (18). In case this is not used as such, the stability conditions would be affected by the time gap h, as also shown in [19]. The origin being an exponentially stable equilibrium of the closed-loop dynamics in (21) implies that all spacing errors $e_i(t)$ converge to zero, thus satisfying the control objective given in (12). The effect of the eigenvalues $\lambda_i\{\hat{L}\}$ on the decay rate of the errors is similar as in [25]

Remark 4: The method used in the proof of Theorem 1 is similar to the line of reasoning in the proof used in [25, Th. 1.3]. However, in this paper, the dynamics involves a velocity-dependent spacing policy and input feedforward.

Remark 5: In [25] and [26], results on fundamental limitations in terms of stability margin for platoon dynamics with constant distance spacing policy are presented. Such result does not yet exist for the platoon dynamics as presented in this paper, in which a constant time gap spacing policy is realized. This can be the topic of the future research.

IV. Consensus-Based Control of a Platoon With Nonhomogeneous Velocity Constraints

In this section, first, a vehicle having a certain maximum velocity $v_{\max}$ is introduced. It is shown that the platoon will break up, under certain conditions, due to this velocity constraint. Second, an additional control law for the virtual reference vehicle is introduced and combined with the consensus-based control law of Section III to regain an exponentially stable equilibrium.

A. Velocity Constraint

In Section III, a homogeneous platoon, consisting of vehicles without velocity constraints, was considered. In this section, a slow (or faulty) vehicle is introduced within the platoon, similar as done in [15], and the platoon dynamics are analyzed in the presence of such an inhomogeneous constraint. Suppose that the maximum velocity of the f^{th} vehicle in the platoon, with $f \in \mathcal{V}$, is defined as $v_{\max}$ such that

$$v_f(t) \leq v_{\max} \quad \forall t. \tag{30}$$

$$\dot{X} = \begin{pmatrix} A - (l_{11} + p_{11})Bk^T & -l_{12}Bk^T & \cdots & -l_{1n}Bk^T \\ -l_{21}Bk^T & \ddots & \ddots & \vdots \\ \vdots & \ddots & \ddots & -l_{(n-1)n}Bk^T \\ -l_{n1}Bk^T & \cdots & -l_{n(n-1)}Bk^T & A - (l_{nn} + p_{nn})Bk^T \end{pmatrix} X \tag{24}$$

Some additional definitions are given to correctly model this saturation on the velocity of vehicle f. Suppose that vehicle f reaches its maximum velocity, i.e., $v_f(t) = v_{\max}$. Then, by definition, the acceleration $a_f(t)$ and desired acceleration $u_f(t)$ are equal to zero, i.e., $a_f(t) = 0$ and $u_f(t) = 0$ if $v_f(t) = v_{\max}$. Given this constraint on the velocity of one of the vehicles in the platoon, one can say that the platoon can have two modes. *Mode* 1 represents normal platoon operation with continuous dynamics as treated in Section III, and *Mode* 2 represents the fixed velocity $v_f(t) = v_{\max}$ for vehicle f and normal operation with continuous dynamics for all other vehicles in the platoon.

In the following, it is shown that when the virtual reference vehicle is uncontrolled, i.e., having constant velocity larger than $v_{\max}$

$$v_0(t) \equiv v_{\text{des}} > v_{\max} \tag{31}$$

with v_{des} being the desired platoon velocity, then the constant platooning velocity solution, investigated in Section III, is not an equilibrium when there is a vehicle f satisfying (30). This is similar as what would occur under such conditions for unidirectional CACC [4], [5].

Let, as a particular case, the communication topology used in the distributed controller $\bar{u}_i(t)$ be defined by the Laplacian matrix

$$L_1 = \begin{pmatrix} 1 & -1 & 0 & \cdots & 0 \\ 0 & \ddots & \ddots & \ddots & \vdots \\ \vdots & \ddots & \ddots & \ddots & 0 \\ \vdots & & \ddots & 1 & -1 \\ 0 & \cdots & \cdots & 0 & 0 \end{pmatrix}. \tag{32}$$

This results in a one-vehicle look-back topology for the implementation of the distributed consensus controller. In addition, a one-vehicle look-forward topology is used for the purpose of feedforward, due to (18). Given the topology of the distributed consensus controller as defined by (32), only the last vehicle in the platoon is the root of a directed spanning tree. Therefore, the pinning element is applied on the last vehicle, that is

$$p_{nn} = 1, \quad p_{ii} = 0 \quad \forall i \neq n. \tag{33}$$

For the analytical derivation of the resulting steady-state solution, it is assumed that when vehicle f goes into saturation, i.e., switches from *Mode* 1 to *Mode* 2, it stays in *Mode* 2.

As a result of the velocity of vehicle f being saturated, and the particular (single vehicle look-back) structure of the topology in (32), the platoon dynamics can be divided into two subsets. The first set $\mathcal{V}_b$ contains all vehicles which drive behind the saturated vehicle, i.e., $\mathcal{V}_b = \{\mathcal{V} | i > f\}$, and the second set $\mathcal{V}_f$ contains all vehicles ahead of the saturated vehicle and the saturated vehicle itself, i.e., all vehicles $\mathcal{V}_f = \{\mathcal{V} | i \leq f\}$. It should be noted that, for this particular topology in (32), for the distributed controller (18) and (20) in combination with the pinning element (33), the last vehicle $i = n$ in the platoon is controlled using unidirectional CACC as presented in [4]. This means that, for vehicle n, the conditions in (27) are the same as in [4]. Hence, the origin is an exponentially stable equilibrium of the error state vector $x_n(t)$ of vehicle $i = n \neq f$, under the condition of a properly designed controller gain vector k.

In Proposition 1, it is stated that under certain conditions, the closed-loop platoon dynamics do not have an equilibrium due to the above-introduced velocity constraint.

Proposition 1: The closed-loop platoon dynamics (21), with the communication topology being defined by (32) and (33) (without loss of generality), do not have a reachable asymptotically stable equilibrium if $v_0(t)$ and $v_f(t)$ satisfy

$$v_f(t) \leq v_{\max} < v_0(t) \equiv v_{\text{des}}. \tag{34}$$

Proof: First, the dynamics of the vehicles behind vehicle f, i.e., subset $\mathcal{V}_b$, are treated. When $v_0(t)$ and $v_f(t)$ satisfy (34), at some point, vehicle f reaches its maximum velocity $v_{\max}$. Clearly, in that mode, vehicle f is not a controlled vehicle, but is driving at constant velocity $v_{\max}$. As a result of the one-vehicle look-back topology for the distributed consensus controller as defined by the Laplacian matrix in (32), when considering all the vehicles in subset $\mathcal{V}_f$, the dynamics of vehicle $f + 1$ depends only on vehicle f. Moreover, with this interaction topology, the dynamics of all other vehicles in vehicle subset $\mathcal{V}_b$ do not depend on any of the vehicles in vehicle subset $\mathcal{V}_f$. Therefore, vehicle f (with $u_f = 0$) acts as a virtual leading vehicle for the vehicles in subset $\mathcal{V}_b$, driving with a constant velocity $v_f = v_{\max}$. Hence, the conditions (27) of Theorem 1 for exponential stability apply for that part of the platoon.

Second, an equilibrium analysis is executed for the dynamics associated with the intervehicle distance error states of the saturated vehicle f and all vehicles ahead of this vehicle, i.e., all vehicles in $\mathcal{V}_f$. In an equilibrium, all time derivatives of the states are equal to zero. For the second time derivative of $e_i(t)$, this equilibrium must satisfy [using (10) and (11)]

$$\ddot{e}_i = a_{i-1} + \frac{h - \tau}{\tau} a_i - \frac{h}{\tau} u_i = 0 \quad \forall i \in \mathcal{V}_f. \tag{35}$$

As stated earlier, the (desired) acceleration of vehicle f is equal to zero when it is in saturation, i.e., $u_f(t) = 0$ and $a_f(t) = 0$. Moreover, there are no restrictions (or saturations) on the vehicles' acceleration $a_i(t)$ or desired acceleration $u_i(t)$ for $i \neq f$. Therefore, (35) has a solution for all $i \in \mathcal{V}_f$, since all vehicles in $\mathcal{V}_f$ (except for vehicle f) can reach $a_i = u_i = 0$ for $t \to \infty$. By using this, and the known relation between the desired acceleration $u_i(t)$ and the actual acceleration $a_i(t)$ as in (11), for $\phi = 0$, it can be shown that the acceleration $a_i(t)$ and the desired acceleration $u_i(t)$ are equal to zero for each vehicle $i \in \mathcal{V}_f$ when (35) holds.

For the first time derivative of $e_i(t)$, the equilibrium must satisfy

$$\dot{e}_i = v_{i-1} - v_i - h a_i = 0 \quad \forall i \in \mathcal{V}_f. \tag{36}$$

As shown earlier, vehicle acceleration $a_i(t)$ equals zero for each vehicle $i \in \mathcal{V}_f$ when the platoon dynamics satisfy (35), i.e., is in a steady state. Employing this fact, (36) results in

$$\begin{aligned} \dot{e}_1 &= v_0 - v_1 = 0 \\ \dot{e}_i &= v_{i-1} - v_i = 0 \quad \forall i \in \{\mathcal{V}_f | 1 < i < f\} \\ \dot{e}_f &= v_{f-1} - v_f = 0. \end{aligned} \tag{37}$$

According to (34) in the proposition, the velocity of the virtual reference vehicle satisfies $v_{\max} < v_0(t) \equiv v_{\text{des}}$ and the velocity of vehicle f satisfies both satisfy $v_f(t) \leq v_{\max}$. As a result, the equilibrium in (37) cannot be reached, and thus, the dynamics of the vehicles in subset $\mathcal{V}_f$ do not have an equilibrium. Hence, Proposition 1 is proven. □

Proposition 1 shows that the platoon will break up in the presence of a limitation on the velocity of one of the vehicles in the platoon, which is lower than the desired velocity imposed by the virtual reference vehicle. In Section IV-B, a controller for the dynamics of the (leading) virtual reference vehicle is introduced and combined with the consensus control law of Section III, to improve the platoon cohesion in the presence of a limit on the velocity of one of the vehicles.

B. Consensus-Based Velocity-Adaptive Platoon Control

As mentioned earlier, the aim of the design of a controller for the virtual reference vehicle is to prevent the platoon from breaking up, even when there is a vehicle in the platoon which has a maximum velocity $v_{\max} < v_{\text{des}}$. In other words, we aim to guarantee that the closed-loop platoon dynamics in (21) still have an exponentially stable equilibrium, associated with a common velocity for all vehicles. The only exogenous input to the closed-loop platoon dynamics in (21) is the desired acceleration of the virtual reference vehicle $u_0(t)$, and therefore, a controller is designed for this input. To arrive at a stable equilibrium, the following control law is proposed for the virtual reference vehicle:

$$\dot{u}_0 = -\frac{1}{h}u_0 + \frac{k_v}{h}(v_{\text{des}} - v_0) - \frac{k_0^T}{h}x_1 \tag{38}$$

where $k_v > 0$ is the velocity control gain, $k_0^T = (k_{p0}\ k_{d0}\ 0)$ are proportional and derivative error controller gains, and $x_1(t)$ is the error state vector of vehicle $i = 1$

$$x_1 = (e_1\ \dot{e}_1\ \ddot{e}_1)^T. \tag{39}$$

One can observe that again a low-pass filter is used having a pole at $-(1/h)$, to have some relaxation effect, such that the desired acceleration of the virtual reference vehicle changes less rapidly. The purpose of the velocity control term in (38) is to drive the velocity of the virtual reference vehicle $v_0(t)$ to the desired platoon velocity $v_{\text{des}}(t)$. The error control term in (38) aims to drive the intervehicle distance error $e_1(t)$ to zero, since it has a negative contribution to the desired acceleration of the virtual reference vehicle. Given the control law for the virtual reference vehicle in (38), the velocity of the virtual reference vehicle $v_0(t)$ is not fixed anymore, i.e., $v_0(t) \not\equiv v_{\text{des}}$. As a result, the equilibrium in (37) may now be reachable.

As mentioned earlier, the platoon can be either in *Mode* 1, i.e., having continuous dynamics for all vehicles in the platoon, or in *Mode* 2, which means that vehicle f is in saturation and all other vehicles have continuous dynamics. In the following, conditions for exponential stability of the platoon dynamics for the separate modes are derived. To this end, in (40), as shown at the bottom of this page, a representation of the entire platoon dynamics is given. This representation is based on the closed-loop platoon dynamics in (21) and, in addition, the dynamics of the virtual reference vehicle subjected to controller (38). Here, matrix A and vector B are as defined in (11), matrix $I_n \in \mathbb{R}^{n\times n}$ is the identity matrix, matrix $I_{(-1),n}$ is defined in (23), matrix $\hat{L} \in \mathbb{R}^{n\times n}$ is defined as $\hat{L} := L + P$, vector $B_u \in \mathbb{R}^{n\times 1}$ is defined in (22), and vector $p_0 = (q_0\ v_0\ a_0)^T$ contains the states of the virtual reference vehicle dynamics. Again, note that switching between the two modes is not taken into account in this stability analysis. The practical relevance of only considering the stability analysis in the individual modes can be understood by realizing that the time scale at which vehicle f goes in and out saturation is typically much slower than the time scale of the closed-loop platoon dynamics. This is realized by assuming that v_{des} changes at a large time scale.

1) Stability in Mode 1: In Theorem 2, conditions for exponential stability of the closed-loop platoon dynamics in (40) will be given.

Theorem 2: The closed-loop platoon dynamics (40), with $\lambda_i\{\hat{L}\} \in \mathbb{R}^+$(positive real) $\forall i \in \mathcal{V}$ and $\tau > 0$, have an exponentially stable steady-state equilibrium (for $\dot{v}_{\text{des}} = 0$) if and only if the controller gain vector k satisfies the conditions in (27), and in addition, controller gain k_v satisfies the condition

$$k_v < \left(\frac{1}{\tau} + \frac{1}{h}\right). \tag{41}$$

Proof: From the dynamical representation in (40), it can directly be seen that $X = 0$ is an exponentially stable equilibrium of the closed-loop error X-dynamics, since the conditions of Theorem 1 are satisfied under the conditions of Theorem 2. Next, from (40), it can be observed that the error state vector $X(t)$ acts as an input to the dynamics of the virtual reference vehicle, i.e., the dynamics regarding the state vector $p_0(t)$ and state $u_0(t)$. These dynamics are defined as follows:

$$\begin{pmatrix} \dot{q}_0(t) \\ \dot{v}_0(t) \\ \dot{a}_0(t) \\ \dot{u}_0(t) \end{pmatrix} = \left(\begin{array}{c|ccc} 0 & 1 & 0 & 0 \\ \hline 0 & 0 & 1 & 0 \\ 0 & 0 & -\frac{1}{\tau} & \frac{1}{\tau} \\ 0 & -\frac{k_v}{h} & 0 & -\frac{1}{h} \end{array}\right) \begin{pmatrix} q_0(t) \\ v_0(t) \\ a_0(t) \\ u_0(t) \end{pmatrix} + \left(\begin{array}{c} 0 \\ \hline 0 \\ 0 \\ B_u^T \otimes -k_0^T \end{array}\right) X(t) + \begin{pmatrix} 0 \\ \hline 0 \\ 0 \\ \frac{k_v}{h} \end{pmatrix} v_{\text{des}}. \tag{42}$$

As mentioned earlier, it is known that $X = 0$ is an exponentially stable equilibrium of the dynamics of the lumped error

$$\begin{pmatrix} \dot{X} \\ \dot{U} \\ \dot{p}_0 \\ \dot{u}_0 \end{pmatrix} = \begin{pmatrix} I_n \otimes A - \hat{L} \otimes Bk^T & O_{3n\times n} & O_{3n\times 3} & O_{3n\times 1} \\ \hat{L} \otimes \frac{k^T}{h} & \frac{1}{h}(I_{(-1),n} - I_n) & O_{n\times 3} & B_u \\ O_{3\times 3n} & O_{3\times n} & A & B \\ B_u^T \otimes -k_0^T & O_{1\times n} & \begin{pmatrix} 0 & \frac{-k_v}{h} & 0 \end{pmatrix} & -\frac{1}{h} \end{pmatrix} \begin{pmatrix} X \\ U \\ p_0 \\ u_0 \end{pmatrix} + \begin{pmatrix} O_{3n\times 1} \\ O_{n\times 1} \\ O_{3\times 1} \\ \frac{k_v}{h} \end{pmatrix} v_{\text{des}} \tag{40}$$

state vector $X(t)$. Exponential stability of the virtual reference vehicle dynamics can thus be assessed by evaluating the poles of the system matrix in (42). The steady-state solution of this system is given by

$$\lim_{t\to\infty}\begin{pmatrix} q_0(t) \\ \hline v_0(t) \\ a_0(t) \\ u_0(t) \end{pmatrix} = \begin{pmatrix} \bar{q}_0(t) \\ \hline v_{\text{des}} \\ 0 \\ 0 \end{pmatrix} \tag{43}$$

where $\bar{q}_0(t) = \int_0^t v_{\text{des}} dt + q_0(0)$ is the position of the virtual reference vehicle in steady state. One eigenvalue of the system matrix in (42) is equal to 0, which is associated with the position state $q_0(t)$. Exponential stability of the steady-state solution can be assessed by evaluating the poles of the lower right submatrix of the system matrix in (42) corresponding to the states $v_0(t)$, $a_0(t)$, and $u_0(t)$. Employing the Routh–Hurwitz stability criterion [23] directly results in the necessary and sufficient conditions for exponential stability of the steady-state solution, as given in (41). What remains, is to check the stability of the subsystem of (40) corresponding to the state vector $U(t)$, i.e., the subsystem

$$\dot{U}(t) = \frac{1}{h}(I_{(-1),n} - I_n)U(t) + \hat{L} \otimes \frac{k^T}{h} X(t) + B_u u_0(t). \tag{44}$$

It has already been shown that $X(t)$ and $u_0(t)$ are zero in steady state. Note that this is called a steady state and not an equilibrium, since the state $q_0(t)$ is not constant in this steady-state solution of the platoon dynamics. Furthermore, matrix $(1/h)(I_{(-1),n} - I_n)$ is a Hurwitz matrix having one eigenvalue

$$\lambda_1 = -\frac{1}{h} \tag{45}$$

with algebraic multiplicity n. Thus, $U = 0$ is an exponentially stable equilibrium of the $U(t)$-subsystem dynamics.

As a result, the platoon dynamics in (40) have an exponentially stable steady-state solution

$$(\bar{X}^T \ \bar{U}^T \ \bar{q}_0 \ \bar{v}_0 \ \bar{a}_0 \ \bar{u}_0)^T = (0^T \ 0^T \ \bar{q}_0(t) \ v_{\text{des}} \ 0 \ 0)^T \tag{46}$$

when the necessary and sufficient conditions in (27) and (41) are satisfied. □

Remark 6: Theorem 2 shows that no conditions on the controller gain vector k_0 are needed for stability. This directly follows from the proof above; moreover, this can be understood by observing that the closed-loop platoon dynamics (40) is lower triangular when partitioning the $X(t)$-dynamics and the other dynamics. The term with gain vector k_0 only appears in the first column of the system matrix in (40), and therefore, there are no conditions on k_0 for stability.

2) Stability in Mode 2: When the platoon is in *Mode 2*, it is assumed that the velocity of vehicle f is constant, i.e., $v_f(t) = v_{\max}$ and $u_f = 0$. With the velocity of vehicle f being constant, vehicle f acts as a leading vehicle with constant velocity for the vehicles behind. Conditions for exponential stability of the dynamics of these vehicles in subset $\mathcal{V}_b$ are given in Section IV-A, while being in *Mode 2*, the stability of the dynamics of the vehicles in subset $\mathcal{V}_f$ is independent of the dynamics of the vehicles in subset $\mathcal{V}_b$.

For the vehicles in the vehicle subset $\mathcal{V}_f$, the constant velocity of vehicle f can be seen as a constant input to the dynamics. To be able to write this constant velocity $v_{\max}$ as a constant input to the system, first, a state transformation must be applied to the dynamics of the vehicle subset $\mathcal{V}_f$ of platoon dynamics representation in (40), such that the vehicle velocity becomes a state. This state transformation will result in a new state representation of the platoon dynamics, in which the vehicles' state vector

$$\chi_i = (e_i \ v_i \ a_i)^T \quad \forall i \in \mathcal{V}_f \tag{47}$$

contains the intervehicle distance error $e_i(t)$, the vehicle velocity $v_i(t)$, and acceleration $a_i(t)$. Similar to the state vectors $x_i(t)$, the state vectors $\chi_i(t)$ are collected in a lumped state vector

$$\chi^T = \begin{pmatrix} \chi_1^T & \cdots & \chi_f^T \end{pmatrix}. \tag{48}$$

Now, let vector $\xi(t)$ be the state vector of the dynamics in (40) excluding the dynamics of the vehicles in the vehicle subset $\mathcal{V}_b$

$$\xi = \begin{pmatrix} (x_1^T & \cdots & x_f^T) & (u_1 & \cdots & u_f) & p_0^T & u_0 \end{pmatrix}^T. \tag{49}$$

The platoon dynamics for vehicle subset $\mathcal{V}_f$ can then be expressed by

$$\dot{\xi} = \mathcal{A}\xi + \mathcal{B}v_{\text{des}} \tag{50}$$

where matrix $\mathcal{A} \in \mathbb{R}^{(4f+4)\times(4f+4)}$ and vector $\mathcal{B} \in \mathbb{R}^{(4f+4)\times 1}$ can be derived from (40). Let a second state vector $\zeta(t)$ be defined as

$$\zeta = \begin{pmatrix} \chi^T & (u_1 & \cdots & u_f) & p_0^T & u_0 \end{pmatrix}^T. \tag{51}$$

Since the vehicle subset dynamics (50) represent a linear time-invariant system, it is known that there exists a similarity transformation matrix $\mathcal{T}$, such that

$$\zeta = \mathcal{T}\xi. \tag{52}$$

More details on this similarity transformation matrix $\mathcal{T}$ can be found in [24]. Applying this similarity transformation to (50) results in

$$\dot{\zeta} = \mathcal{T}\mathcal{A}\mathcal{T}^{-1}\zeta + \mathcal{T}\mathcal{B}v_{\text{des}}. \tag{53}$$

As a second step, the velocity $v_f(t)$, acceleration $a_f(t)(\equiv 0)$, and desired acceleration $u_f(t)(\equiv 0)$ can be removed from the state space of the platoon dynamics, since $v_f(t) = v_{\max}$ is assumed to be constant. As a result, the dynamics of the intervehicle distance error of vehicle f is given by

$$\dot{e}_f(t) = v_{f-1}(t) - v_{\max}. \tag{54}$$

Consequently, the states $v_f(t)$, $a_f(t)$, and $u_f(t)$ can be removed from the state space in (53). This results in the following state vector of the platoon dynamics:

$$\rho = \begin{pmatrix} \chi_1^T & \cdots & \chi_{f-1}^T & e_f & U_r^T & p_0^T & u_0 \end{pmatrix}^T \tag{55}$$

where $U_r(t) = (u_1(t) \ \cdots \ u_{f-1}(t))^T$. Thus, the order of the platoon dynamics (53) is reduced with three. The platoon dynamics can now be represented by

$$\dot{\rho} = \mathcal{A}_R\rho + \mathcal{B}_{R,1}v_{\max} + \mathcal{B}_{R,2}v_{\text{des}} \tag{56}$$

where system matrix $\mathcal{A}_R$, vector $\mathcal{B}_{R,1}$, and vector $\mathcal{B}_{R,2}$ have a complex structure which can be found in [24].

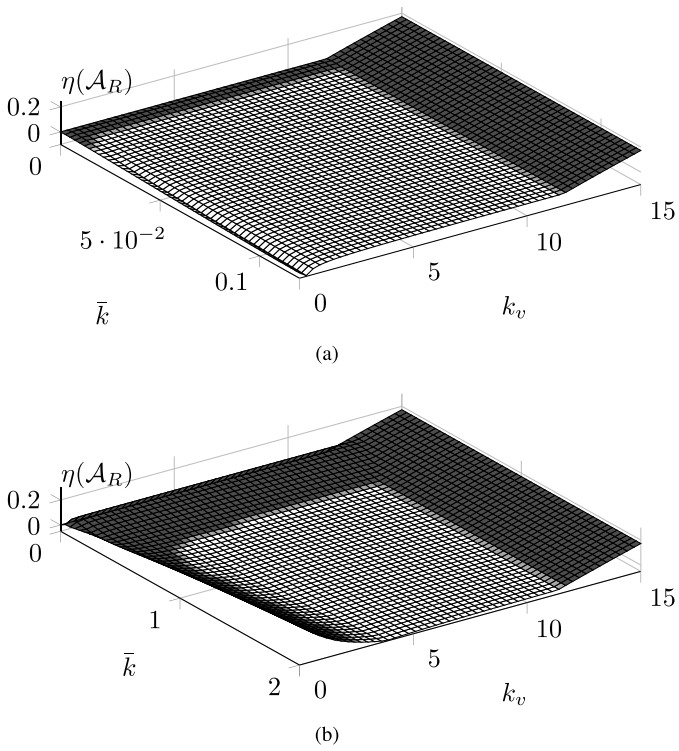

Fig. 2. Maximum of the real part of the eigenvalues of matrix $\mathcal{A}_R$, i.e., $\eta(\mathcal{A}_R)$ (for $\alpha = 5$). Dark gray indicates that the maximum is larger than zero, which results in unstable platoon dynamics. (a) $f = 3$. (b) $f = 10$.

In (56), the maximum velocity $v_{\max}$ and the desired platoon velocity $v_{\text{des}}(t)$ are now both written as external inputs to the platoon dynamics. The steady-state solution of (56) is given as

$$\bar{\rho} = \left(\bar{1}_{1\times(f-1)} \otimes (\bar{e}\ v_{\max}\ 0)\ \ \bar{e}\ O_{1\times(f-1)}\ \bar{q}_0(t)\ v_{\max}\ 0\ 0\right)^T \quad (57)$$

where vector $\bar{1}_{1\times(f-1)} \in \mathbb{R}^{1\times(f-1)}$ only contains elements being equal to one, vector $O_{1\times(f-1)} \in \mathbb{R}^{1\times(f-1)}$ is a zero vector, and $\bar{e} = (k_v/k_{p0})(v_{\text{des}} - v_{\max})$.

In contrast to the system matrix in (40), the structure of system matrix $\mathcal{A}_R$ does not allow for the derivation of analytical conditions for exponential stability of the platoon dynamics. Therefore, only numerical results are given on exponential stability of the dynamics in (56). In Fig. 2, the maximum of the real part of the eigenvalues of matrix $\mathcal{A}_R$ is plotted against control gain k_v and gain $\bar{k}$, where the controller gains are chosen as

$$k_1 = \bar{k}, \quad k_2 = \alpha\bar{k}, k_3 = 0, \quad k_p = \bar{k}, \quad k_d = \alpha\bar{k}. \quad (58)$$

This design for the controller gains leaves two degrees of freedom, namely, k_v and k, where k_v is associated with the platoon trying to reach its desired velocity and k mainly influences the interaction between the vehicles. This two-degree of freedom structure allows for providing insight on the platoon stability using a 3-D plot, as shown in Fig. 2. The time gap used here is defined as $h = 0.6$ s. The dark gray area of the surface plot indicates the instability of the platoon dynamics. One can clearly see the stability boundary defined by the condition in (41), which is a condition related to the dynamics of the virtual reference vehicle (42). This condition for exponential stability does indeed not depend on the platoon length, as can be seen by comparing the maximum real eigenvalue plot for a platoon with $f = 3$ and $f = 10$, i.e., the third or tenth vehicle is saturated in velocity. Nevertheless, by comparing Fig. 2(a) and (b), one can observe that increasing the index f of the vehicle being saturated in velocity does decrease the size of the set of controller gains that result in exponentially stable platoon dynamics. This effect is related to the amount of vehicles situated ahead of the saturated vehicle, which influences the system matrix $\mathcal{A}_R$ in (56).

Remark 7: This means that if in practice you do not know where in the platoon the saturated vehicle will be, a careful design of the controller parameters is in order accounting for the maximum number of vehicles ahead of a potentially saturating vehicle.

However, from Fig. 2(b), it can be observed that for controller gains: $3 < k_v < 11.4$ and $0.56 < k < 2$, the platoon dynamics is exponentially stable for a platoon up to ten vehicles, with the minimum velocity constraint being present on any arbitrary vehicle in the platoon.

In this paper, only a single vehicle velocity constraint is assumed to be present in the platoon. In case there are multiple vehicles in the platoon which are, possibly differently, constrained in velocity, the velocity in the equilibrium of the platoon dynamics will be equal to the maximum velocity of the slowest constrained vehicle. Asymptotic stability of this equilibrium depends on many conditions; for example, the amount of vehicles that are in between these constrained vehicles. However, multivehicle constraints are not investigated in this paper.

V. Simulation Results

In this section, first, numerical simulations are executed to validate the main exponential stability result obtained in Section III.

In these simulations, the vehicle parameters are set to $\tau = 0.1$ s and $l_v = 4.46$ m, and the desired spacing-policy parameters are set to $r = 2$ m and $h = 1$ s. As was mentioned earlier, during the control law design, it was assumed that the actuator delay ϕ is equal to zero. Also, until now, it is assumed that the wireless communication between the vehicles is not subjected to delay. However, the influence of both of these delays cannot be ignored in practice. Therefore, additional simulations are executed as a comparison, having an actuator delay of $\phi = 0.2$ s and a communication delay of $\theta = 0.02$ s, which are typical values for a practical setup as will be described in the following. The signals that are received through wireless communication, i.e., $u_{i-1}(t)$ and $x_j(t)$, are subject to this communication delay θ. The communication topology used in the distributed control term $\bar{u}_i(t)$ is defined by the Laplacian matrix as defined in (32), and the pinning matrix being defined as in (33), such that the positive real assumption on the eigenvalues of $\hat{L}$ in Theorem 1 is satisfied. The controller gain vector is chosen as $k^T = (0.2\ 1.2\ 0)$, which satisfies the conditions for exponential stability as given in Theorem 1 while yielding a reasonable transient response in terms of settling time and comfort. The control gain $k_{dd} = 0$ is chosen, since feedback of the jerk error is in practice

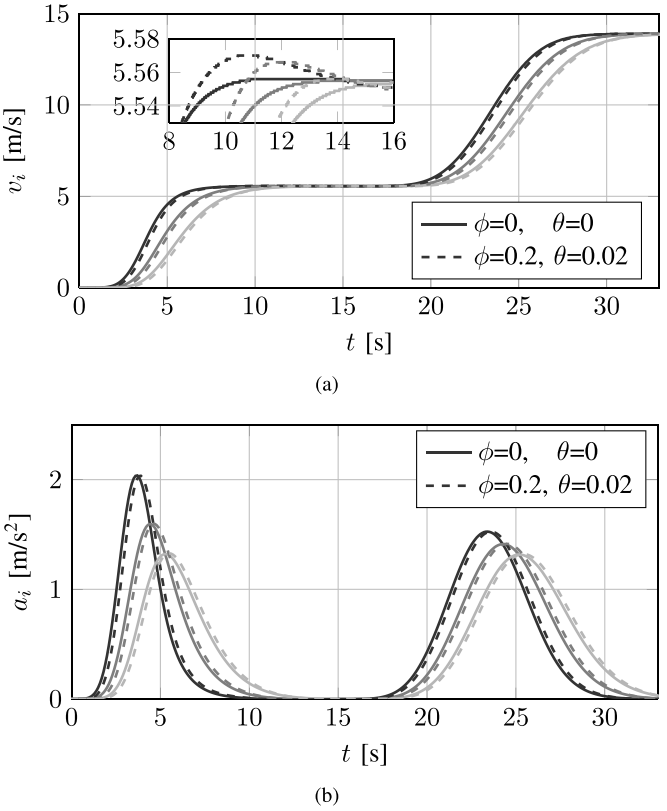

Fig. 3. Simulated time response of (a) velocity $v_i(t)$ and (b) acceleration $a_i(t)$ (dark-light gray: $i = 1, 2, 3$), with zero delays and nonzero delays $\phi = 0.2$ s and $\theta = 0.02$ s.

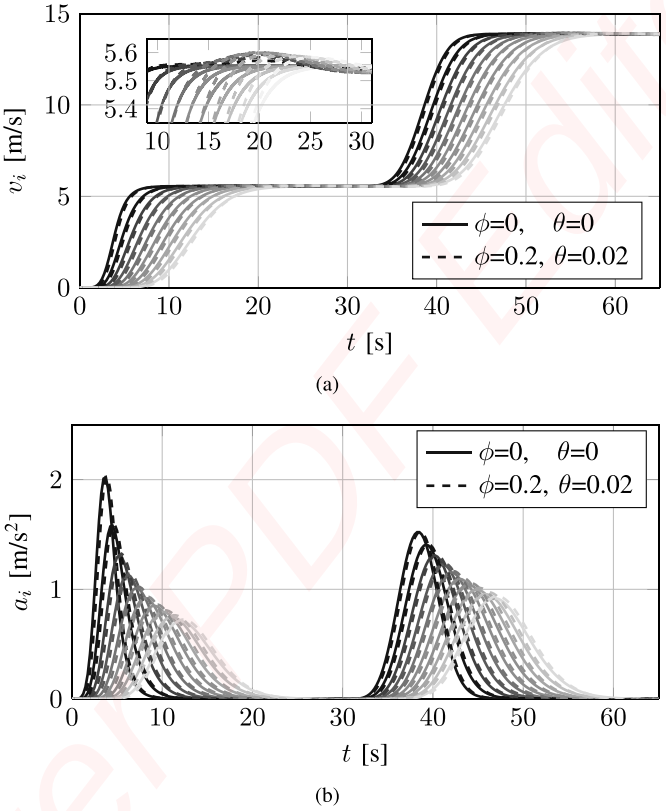

Fig. 4. Simulated time response of (a) velocity $v_i(t)$ and (b) acceleration $a_i(t)$ (dark-light gray: $i = 1, 2, \cdots, 10$), with zero delays and nonzero delays $\phi = 0.2$ s and $\theta = 0.02$ s.

unfeasible due to high measurement noise. A simulation study is executed using a prescribed smooth step velocity profile for $v_0(t)$, based on which the input $u_0(t)$ has been calculated. Initially, the platoon is at standstill in equilibrium. The height of the first and second smooth step in velocity is 5.56 m/s (20 km/h) and 8.33 m/s (30 km/h), respectively, such that eventually the platoon is driving at 13.89 m/s (50 km/h). Fig. 3 shows the velocity and acceleration responses for a platoon of three vehicles, i.e., $n = 3$. In addition to the simulation with zero delay, the platoon response for the case with actuator delay $\phi = 0.2$ s and communication delay $\theta = 0.02$ s is presented. One can observe that the platoon dynamics are exponentially stable and that all vehicles in the platoon follow the velocity profile imposed by the virtual reference vehicle for both scenarios. When comparing the platoon responses with delays and without delays, one can observe that the responses are comparable; however, the response with delays is slightly slower. Moreover, a slight overshoot is observed in the velocity response compared with the response with zero delays (visible in zoomed-in view of Fig. 3); However, for both scenarios, no overshoot with respect to the predecessor is present in the velocity response. Furthermore, the maximum amplitude of the acceleration response decreases for increasing vehicle index i for both scenarios, as can be seen in Fig. 3(b). That is, in upstream direction of the platoon, we see the desired behavior in terms of input disturbance attenuation. The intervehicle distance errors $e_i(t)$ also converge to zero, although this is not explicitly shown here.

Although string stability [4] is not extensively assessed here, the influence of the platoon length n on the platoon response is evaluated by applying the same "double smooth step" velocity profile to a platoon of length $n = 10$ vehicles. The only difference is an additional phase of 15 s in between the two smooth steps, such that the second smooth step starts when the transients due to the first step are approximately vanished. In Fig. 4, the resulting platoon responses for a platoon of length $n = 10$ vehicles are shown for zero and nonzero delays ϕ and θ. Similar to the case of the platoon of length $n = 3$, the intervehicle distance errors $e_i(t)$ converge to zero for both scenarios. When comparing the simulations with nonzero delays and zero delays, again the responses are comparable. However, for nonzero delays, the responses are again slower and a slight overshoot is observed compared with the velocity responses with no delay. Now, in contrast to a platoon of length $n = 3$, a minor overshoot with respect to the predecessor occurs in the velocity response for some of the vehicles in the platoon (visible in zoomed-in view of Fig. 4). Namely, for the vehicles $i \in \{2, 3, 4, 5\}$, a slight overshoot in the velocity response is observed with respect to their preceding vehicles, see inset in Fig. 4(a), suggesting string unstable behavior. However, for the acceleration response, still a decreasing trend of the maximum value in the upstream direction of the platoon is present, as is visible in Fig 4(b).

For larger platoon lengths, for example, platoon lengths above $n = 20$ vehicles, the overshoot with respect to the desired equilibrium velocity is more than 1% of the smooth step height (approximately). Also, more oscillatory behavior

occurs around the equilibrium velocity, and thus, increasing the platoon length n leads to less damped transient behavior, again suggesting string unstable behavior. As it can be seen through the simulation results, due to the bidirectional nature of the interaction between the vehicles in the platoon, changing the platoon length n influences the dynamical behavior of all vehicles in the platoon (although in accordance with Theorem 1, closed-loop platoon stability will remain guaranteed for any platoon length). As a result, assessment of performance properties such as disturbance attenuation in relation to the platoon length n (related to string stability) is not straightforward. For example, the method for finding a minimal time headway h that guarantees string stability as described in [28] does not apply for bidirectionally connected systems. Alternatively, one could analyze string stability using a passivity-based framework, such as presented in [30]. However, that result should be then extended to velocity-dependent spacing policy. From this, it is clear that the analysis of string stability is not straightforward, and therefore, an extensive analysis of the influence of the platoon (or string) length on string stability for such bidirectional network topologies is left for future research.

Remark 8: Similarly, as for an increase in platoon length n, for a decrease in the desired time gap h, the overshoot in the velocity response shows a slightly increasing trend.

As mentioned in Section III, the decay rate of an initial condition perturbation depends on the eigenvalues of the Laplacian matrix L. To illustrate this effect, the transient response for an initial condition perturbation for two different topologies is compared. The first topology is the same as used in the simulations shown earlier, i.e., a one vehicle look-back topology defined by (32) and (33). The second topology is defined by the Laplacian matrix

$$L_2 = \begin{bmatrix} 1 & -1 & 0 & \dots & 0 \\ -1 & 2 & \ddots & & \vdots \\ 0 & \ddots & \ddots & \ddots & 0 \\ \vdots & & \ddots & 2 & -1 \\ 0 & \dots & 0 & -1 & 1 \end{bmatrix} \tag{59}$$

characterizing a bidirectional topology, and the following pinning element:

$$p_{11} = 1, \qquad p_{ii} = 0 \quad \forall i \neq 1. \tag{60}$$

Initially, all the vehicles in the platoon have a spacing error $e_i(0)$ with respect to the steady-state zero value. The transient response for both topologies is shown in Fig. 5. It can be observed that for the first topology, i.e., Topology 1, the initial condition perturbation is damped out after approximately 40 s. In contrast, for Topology 2, the initial condition perturbation is not yet damped out after 100 s. This can be explained by observing the second smallest eigenvalue of the Laplacian matrices of both topologies, which are

$$\begin{aligned} &\text{Topology 1:} \quad \lambda_2\{L_1\} = 1 \\ &\text{Topology 2:} \quad \lambda_2\{L_2\} = 0.098. \end{aligned}$$

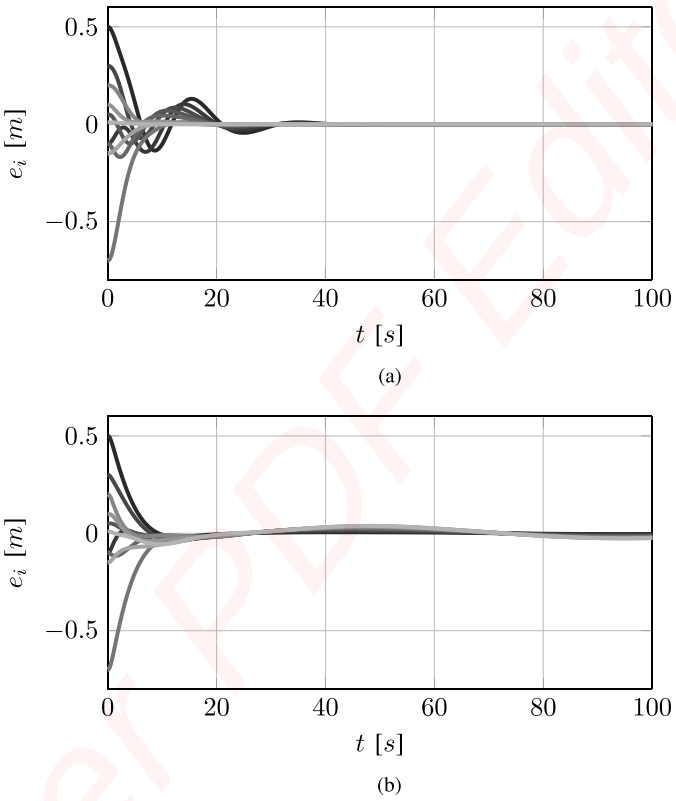

Fig. 5. Spacing error $e_i(t)$ response for two different communication topologies for the distributed feedback controller (dark-light gray: $i = 1, 2, \cdots, 10$), with zero delays. (a) Topology 1 (one vehicle look-back). (b) Topology 2 (one vehicle look-back and look-forward).

The significantly lower second smallest eigenvalue for Topology 2 explains the smaller decay rate for this topology in the simulation. Similar to the reasoning presented in [25], when the platoon length n goes to infinity, for Topology 2, the second smallest eigenvalue approaches zero. However, the method proposed in this paper is meant for the improvement of cohesion between vehicles in a platoon with a relatively small finite platoon length. Nevertheless, the communication topology defined by L and P must be designed carefully. In the remainder of this paper, only Topology 1 is considered.

Next, numerical simulation results are shown to demonstrate the adaptability of the platoon to a velocity constrained vehicle under the bidirectional interaction control structure. In this simulation, the same structure is used for the distributed controller, i.e., the communication topology is defined by (32) and the pinning element by (33). Suppose the desired platoon velocity v_{des}, imposed by the controller of the virtual reference vehicle as given in (38), is 13.89 m/s (50 km/h). A simulation of a platoon of three vehicles is described. Here, the focus is on a three-vehicle platoon to be able to compare the result with the experimental results described in Section VI. The velocity of the third vehicle in the platoon is limited to a maximum of $v_{\max} = 9.72$ m/s (35 km/h). Fig. 6 shows the platoon response for this platoon configuration. It can be observed that the initial velocity of the vehicles in the platoon is approximately 5 m/s (18 km/h). Since this is lower than the desired velocity imposed by the virtual reference vehicle,

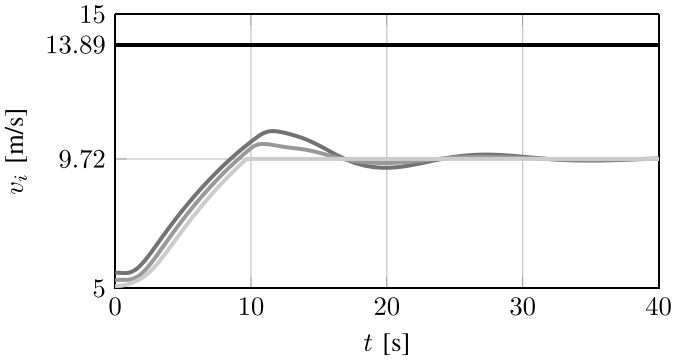

Fig. 6. Simulated time response of the velocity for a platoon of three vehicles, including a vehicle having limited velocity (black: desired velocity v_{des} and dark-light gray: $i = 1, 2, 3$).

Fig. 7. Experimental three-passenger vehicle platoon.

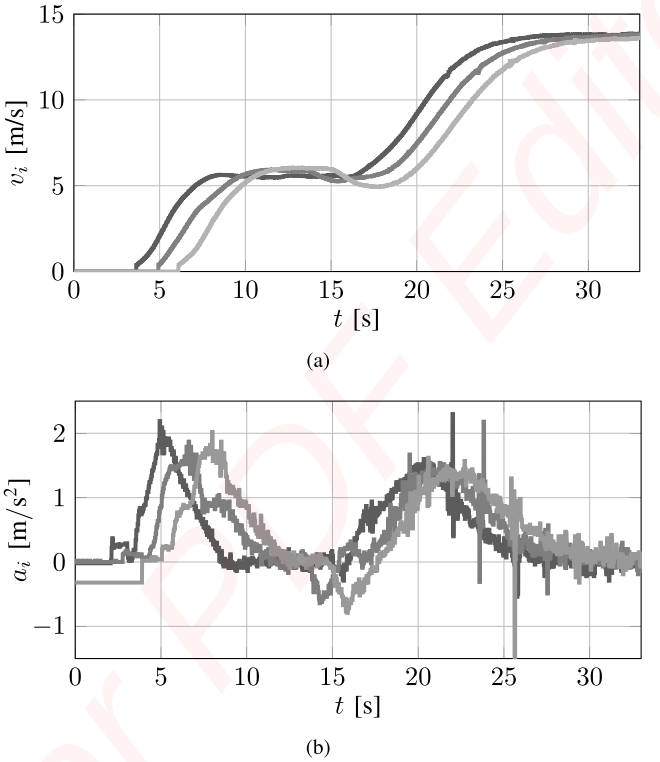

Fig. 8. Measured time response of (a) velocity $v_i(t)$ and (b) acceleration $a_i(t)$ (dark-light gray: $i = 1, 2, 3$).

the vehicles in the platoon start to increase their velocity. After approximately 10 s, the third vehicle in the platoon has reached its maximum velocity. It can be observed that the first vehicle initially strives to increase its velocity to the desired velocity v_{des}; however, at some point, the influence of the look-back structure in the consensus-based control approach is visible. As a result, the first and the second vehicle will adapt their velocity according to the maximum velocity of this limited third vehicle, such that the platoon does not break up.

Suppose that the platoon would have a length of ten vehicles, such that there are seven vehicles driving behind the constrained third vehicle. The velocity of those seven vehicles would also converge to this maximum velocity $v_{\max}$.

VI. Experimental Results

To demonstrate the practical feasibility of the proposed consensus-based control strategy, the distributed controller in (18) and (20) is implemented in three longitudinally automated passenger vehicles (Toyota Prii). Each vehicle is equipped with on-board radar and camera sensors to measure the longitudinal distance toward the preceding vehicle, and in addition, IEEE 802.11p-based wireless intervehicle communication is used. The longitudinal dynamics of the automated passenger vehicles, which are shown in Fig. 7, have been identified to comply with (11), with $\tau = 0.1$ s and $\phi = 0.2$ s. The hardware implementation is identical to the one described in [4]. Based on the earlier experiments, it is known that the communication of the desired vehicle acceleration $u_{i-1}(t)$ and consensus state vector(s) $x_j(t)$ to a vehicle i is subjected to a communication delay of $\theta \approx 0.02$ s. Furthermore, the platoon input $u_0(t)$ and all controller parameters are chosen the same as in the above-described simulation study. The measured responses of the executed test scenario are shown in Fig. 8. When comparing the measured response of this experimental test and the simulated response in Fig. 3, it can be observed that, besides the presence of noise in case of the experimental results, the responses are comparable. These results confirm that the proposed consensus-based control strategy indeed induces exponentially stable platoon dynamics. For the measured velocity response, some overshoot is visible after the first smooth step; however, this may be caused by unmodeled disturbance effects. During the second smooth step, one can clearly see the similarities in simulated and experimental responses. When comparing the acceleration responses, obviously the measured acceleration responses are contaminated with noise; however, the shape and amplitude of the simulated and measured acceleration are comparable.

Next, experimental results are shown to demonstrate the practical feasibility of the proposed consensus-based control strategy to improve a platoon's cohesion, i.e., enabling platoon adaptability to a velocity constrained vehicle. The initial platoon conditions and designed parameters, such as controller gains, desired platoon velocity, and platoon length, in this experimented scenario are similar to those used in the platoon adaptability simulation of which the response was shown in Fig. 6. The results of the practical experiments are shown in Fig. 9. It can be observed that the initial platoon velocity is again below the desired velocity v_{des}. The vehicles in the platoon start to increase their velocity until the third vehicle reaches its maximum velocity $v_{\max}$, and the vehicles adapt their velocity accordingly. When comparing the simulated response as shown in Fig. 6 and the experimentally obtained response shown in Fig. 9, one can see that these responses are

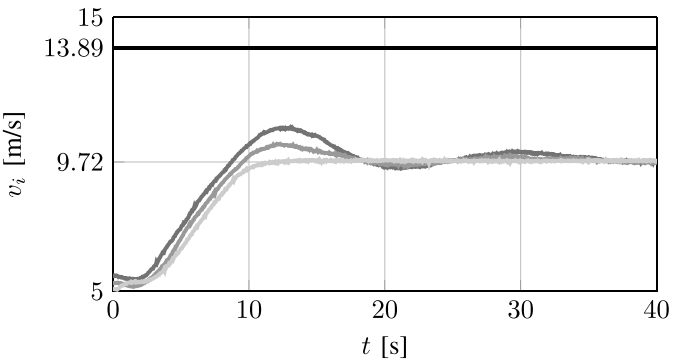

Fig. 9. Measured time response of the velocity for a platoon of three vehicles, including a vehicle having limited velocity (black: desired velocity v_{des} and dark-light gray: $i = 1, 2, 3$).

very similar. This shows, in addition to the practical feasibility of the approach, that the modeling of the simulation-based study is done in a representative way.

In summary, the presented experimental results, first, demonstrate the feasibility of the proposed consensus-based control strategy for vehicular platooning in practice. Improvement of the platoon cohesion, in the sense of automatic velocity adaptation to a velocity constrained vehicle, is verified as well. Second, the experimental results show a good correspondence with the model-based simulation results, thereby motivating further work in the direction of model-based design of consensus strategies for platooning systems.

VII. Conclusion

A novel distributed consensus control approach for longitudinal vehicular platoon control has been proposed. Within this approach, a realistic model is used for the vehicle's longitudinal dynamics and a velocity-dependent spacing policy for consecutive vehicles is employed. With the proposed controllers and subject to a bidirectional connectivity pattern, the adaptability of platoon members to vehicles with velocity constraints is formally proven. This adaptability of the platoon members' velocity is dealt with/without the use of a switching controller or decision logic. Conditions for the exponential platoon stability of the resulting closed-loop dynamics have been formulated. The control approach is validated in practice by applying it to a platoon of three passenger vehicles. In this paper, the dynamical behavior for one communication topology using the designed distributed control is evaluated. Evaluation of the influence of the communication topology on the dynamical behavior is a relevant topic, which will be addressed in the future work. Moreover, further research should also investigate string stability properties of platooning systems with other topologies than unidirectional interaction topologies.

References

[1] S. E. Shladover, "Automated vehicles for highway operations (automated highway systems)," *Proc. Inst. Mech. Eng., I, J. Syst. Control Eng.*, vol. 219, no. 1, pp. 53–75, Nov. 2005.

[2] T. Sachse, O. Grabner, M. Mockel, C. Kaschwich, and J. Plattner, "Intelligent traffic control and optimization with cooperative systems on the eHighway: Using the electrified highway-infrastructure for heavy good vehicles and the advanced traffic control center with V2X for a more efficient and safer traffic (for all road users)," in *Proc. Int. Conf. Connected Vehicles Expo*, Nov. 2014, pp. 558–564.

[3] F. Morbidi, P. Colaneri, and T. Stanger, "Decentralized optimal control of a car platoon with guaranteed string stability," in *Proc. Eur. Control Conf.*, Jul. 2013, pp. 3494–3499.

[4] J. Ploeg, N. van de Wouw, and H. Nijmeijer, "Lp string stability of cascaded systems: Application to vehicle platooning," *IEEE Trans. Control Syst. Technol.*, vol. 22, no. 2, pp. 786–793, Mar. 2014.

[5] K. Lidström *et al.*, "A modular CACC system integration and design," *IEEE Trans. Intell. Transp. Syst.*, vol. 13, no. 3, pp. 1050–1061, Sep. 2012.

[6] V. Milanès, S. E. Shladover, J. Spring, C. Nowakowski, H. Kawazoe, and M. Nakamura, "Cooperative adaptive cruise control in real traffic situations," *IEEE Trans. Intell. Transp. Syst.*, vol. 15, no. 1, pp. 296–305, Feb. 2014.

[7] R. Olfati-Saber and R. M. Murray, "Consensus problems in networks of agents with switching topology and time-delays," *IEEE Trans. Autom. Control*, vol. 49, no. 9, pp. 1520–1533, Sep. 2004.

[8] R. Olfati-Saber, "Flocking for multi-agent dynamic systems: Algorithms and theory," *IEEE Trans. Autom. Control*, vol. 51, no. 3, pp. 401–420, Mar. 2006.

[9] Y. Cao, W. Yu, W. Ren, and G. Chen, "An overview of recent progress in the study of distributed multi-agent coordination," *IEEE Trans. Ind. Informat.*, vol. 9, no. 1, pp. 427–438, Feb. 2013.

[10] M. di Bernardo, A. di Salvi, and S. Santini, "Distributed consensus strategy for platooning of vehicles in the presence of time-varying heterogeneous communication delays," *IEEE Trans. Intell. Transp. Syst.*, vol. 16, no. 1, pp. 102–112, Feb. 2015.

[11] U. Montanaro, M. Tufo, G. Fiengo, M. di Bernardo, A. Salvi, and S. Santini, "Extended cooperative adaptive cruise control," in *Proc. IEEE Intell. Veh. Symp.*, Jun. 2014, pp. 605–610.

[12] Y. Zheng, S. E. Li, J. Wang, L. Y. Wang, and K. Li, "Influence of information flow topology on closed-loop stability of vehicle platoon with rigid formation," in *Proc. 17th Int. IEEE Conf. Intell. Transp. Syst.*, Oct. 2014, pp. 2094–2100.

[13] J. P. Maschuw, G. C. Keßler, and D. Abel, "LMI-based control of vehicle platoons for robust longitudinal guidance," in *Proc. 17th IFAC World Congr.*, Jul. 2008, pp. 12111–12116.

[14] R. Rajamani and C. Zhu, "Semi-autonomous adaptive cruise control systems," *IEEE Trans. Veh. Technol.*, vol. 51, no. 5, pp. 1186–1192, Sep. 2002.

[15] E. Semsar-Kazerooni and K. Khorasani, "Optimal performance of a modified leader-follower cooperative team with partial availability of the leader command and agents actuator faults," in *Proc. IEEE Conf. Decision Control*, Dec. 2007, pp. 2491–2497.

[16] Z. Bo, W. Wei, and Y. Hao, "Distributed consensus tracking control of linear multi-agent systems with actuator faults," in *Proc. IEEE Conf. Control Appl.*, Oct. 2014, pp. 2141–2146.

[17] W. Ren, "On consensus algorithms for double-integrator dynamics," in *Proc. IEEE Conf. Decision Control*, Dec. 2007, pp. 2295–2300.

[18] J. C. Zegers, E. Semsar-Kazerooni, J. Ploeg, N. van de Wouw, and H. Nijmeijer, "Consensus-based bi-directional CACC for vehicular platooning," in *Proc. IEEE Amer. Control Conf.*, Jul. 2016, pp. 2578–2584.

[19] G. J. L. Naus, R. P. A. Vugts, J. Ploeg, M. J. G. van de Molengraft, and M. Steinbuch, "String-stable CACC design and experimental validation: A frequency-domain approach," *IEEE Trans. Veh. Technol.*, vol. 59, no. 9, pp. 4268–4279, Nov. 2010.

[20] X. Li, X. Wang, and G. Chen, "Pinning a complex dynamical network to its equilibrium," *IEEE Trans. Circuits Syst. I, Reg. Papers*, vol. 51, no. 10, pp. 2074–2087, Oct. 2004.

[21] W. Ren and R. Beard, *Distributed Consensus in Multi-Vehicle Cooperative Control*. London, U.K.: Springer-Verlag, 2008.

[22] J. A. Fax and R. M. Murray, "Information flow and cooperative control of vehicle formations," *IEEE Trans. Autom. Control*, vol. 49, no. 9, pp. 1465–1476, Sep. 2004.

[23] A. Hurwitz, "On the conditions under which an equation has only roots with negative real parts," *Sel. Papers Math. Trends Control Theory*, vol. 46, no. 2, pp. 273–284, 1964.

[24] J. C. Zegers, "Distributed consensus control in vehicle platooning," M.S. thesis, Dept. Mech. Eng. Dyn. Control, Eindhoven Univ. Technol., Eindhoven, The Netherlands, May 2015. [Online]. Available: http://alexandria.tue.nl/extra2/afstversl/W_OpenAccess/Zegers_2015.pdf

[25] Y. Zheng, S. E. Li, J. Wang, L. Y. Wang, and K. Li, "Stability and scalability of homogeneous vehicular platoon: Study on the influence of information flow topologies," *IEEE Trans. Intell. Transp. Syst.*, vol. 17, no. 1, pp. 14–26, Jan. 2016.

[26] Y. Zheng, S. E. Li, K. Li, and L.-Y. Wang, "Stability margin improvement of vehicular platoon considering undirected topology and asymmetric control," *IEEE Trans. Control Syst. Technol.*, vol. 24, no. 4, pp. 1253–1265, Jul. 2016.
[27] S. E. Li, Y. Zheng, K. Li, and J. Wang, "An overview of vehicular platoon control under the four-component framework," in *Proc. IEEE Intell. Vehicle Symp.*, Jun./Jul. 2015, pp. 286–291.
[28] S. Klinge and R. H. Middleton, "Time headway requirements for string stability of homogeneous linear unidirectionally connected systems," in *Proc. Joint 48th IEEE Conf. Decision Control 28th Chin. Control Conf.*, Dec. 2009, pp. 1992–1997.
[29] P. Barooah and J. P. Hespanha, "Error amplification and disturbance propagation in vehicle strings with decentralized linear control," in *Proc. Joint 44th IEEE Conf. Decision Control Eur. Control Conf.*, Dec. 2005, pp. 4964–4969.
[30] S. Knorn, A. Donaire, J. C. Agüero, and R. H. Middleton, "Passivity-based control for multi-vehicle systems subject to string constraints," *Automatica*, vol. 12, pp. 3224–3230, Dec. 2014.

Jeroen C. Zegers received the M.Sc. degree in mechanical engineering (Hons.) from the Eindhoven University of Technology, Eindhoven, The Netherlands, in 2015.

Since 2015, he has been with TNO, Helmond, The Netherlands, where he is currently a Research Scientist. His current research interests include modeling and control of nonlinear dynamical systems, and design and analysis of cooperative control systems for heterogeneous vehicular platooning and lateral vehicle motion control.

Elham Semsar-Kazerooni received the Ph.D. degree from Concordia University, Montréal, QC, Canada, in 2009, with a focus on cooperative control of multiagent systems.

She was an FQRNT Researcher with the University of Toronto, Toronto, ON, USA, from 2009 to 2012, where she was involved in reachability analysis and transient control of hybrid systems. She is currently a Senior Research Scientist with the Integrated Vehicle Safety Department, TNO, Helmond, The Netherlands. She has a part-time affiliation with the Department of Applied Mathematics, University of Twente, Enschede, The Netherlands. She is an Author of the book *Team Cooperation in a Network of Multi-Vehicle Unmanned Systems: Synthesis of Consensus Algorithms* (Springer–Verlag, 2012). Her current research interests include multilayered architecture design for automated driving applications, cooperative control design for heterogeneous platoons, and design of interaction protocols for complex driving scenarios.

Jeroen Ploeg received the M.Sc. degree in mechanical engineering from the Delft University of Technology, Delft, The Netherlands, in 1988, and the Ph.D. degree in mechanical engineering on the control of vehicle platoons from the Eindhoven University of Technology, Eindhoven, The Netherlands, in 2014.

From 1989 to 1999, he was with Koninklijke Hoogovens (currently Tata Steel), IJmuiden, The Netherlands, where he was involved in the development and implementation of dynamic process control systems for large-scale industrial plants. Since 1999, he has been with TNO, Helmond, The Netherlands, where he is currently a Principal Scientist. He also has a part-time affiliation with the Mechanical Engineering Department, Eindhoven University of Technology, Eindhoven, The Netherlands. His current research interests include control system design for cooperative and automated vehicles, in particular string stability of vehicle platoons, the design of interaction protocols for complex driving scenarios, and motion control of wheeled mobile robots.

Nathan van de Wouw was born in 1970. He received the M.Sc. degree (Hons.) and Ph.D. degree in mechanical engineering from the Eindhoven University of Technology, Eindhoven, The Netherlands, in 1994 and 1999, respectively.

He holds a full professor position with the Mechanical Engineering Department, Eindhoven University of Technology. He also holds an adjunct full professor position with the University of Minnesota, Minneapolis, MN, USA, and a (part-time) full professor position with the Delft University of Technology, Delft, The Netherlands. In 2000, he has been with Philips Applied Technologies, Eindhoven. In 2001, he was with the Netherlands Organisation for Applied Scientific Research (TNO), Delft. He has held positions as a Visiting Professor with the University of California at Santa Barbara, Santa Barbara, CA, USA, in 2006 and 2007, the University of Melbourne, Melbourne, VIC, Australia, in 2009 and 2010, and the University of Minnesota, in 2012 and 2013. He has published a large number of journal and conference papers and the books *Uniform Output Regulation of Nonlinear Systems: A convergent Dynamics Approach* with A.V. Pavlov and H. Nijmeijer (Birkhauser, 2005) and *Stability and Convergence of Mechanical Systems with Unilateral Constraints* with R.I. Leine (Springer-Verlag, 2008). His current research interests include modeling analysis and control of nonlinear/hybrid systems, with applications to vehicular platooning, high-tech systems, resource exploration, smart energy systems, and networked control systems.

Dr. van de Wouw received the IEEE Control Systems Technology Award for the development and application of variable-gain control techniques for high-performance motion systems in 2015. He is currently an Associate Editor of the *Automatica* and the *IEEE Transactions on Control Systems Technology*.

Henk Nijmeijer (F'00) was born in 1955.

He is currently a Full Professor and the Chair of the Dynamics and Control Group of the Mechanical Engineering Department at Eindhoven University of Technology. He has published a large number of journal and conference papers, and several books, and is or was at the editorial board of numerous journals.

Mr. Nijmeijer has been an IFAC Council Member since 2011. He was a recipient of the 2015 IEEE Control Systems Technology Award. He is also a Program Leader of the Dutch Research Program Integrated Cooperative Automated Vehicles, Eindhoven. He received the IEE Heaviside Premium in 1990. He is also an Editor of Communications in nonlinear science and numerical simulations. He is appointed honorary knight of the golden feedback loop, Norwegian University of Science and Technology, in 2011. In 2015, he was the Scientific Director of the Dutch Institute of Systems and Control, Delft/Eindhoven.